The Dichotomy of the Galactic Halo of the Milky Way

D. Carollo[1,2], T. C. Beers[2], M. Chiba[6], J. E. Norris[4], R. Wilhelm[3], Y.S. Lee[2], T. Sivarani[2], B. Marsteller[2], C. Allende Prieto[3], J.A. Munn[5]

[1]INAF-OATo, [2] Michigan State Univ./JINA, [3]Univ. of Texas, [4]Australian National Univ., [5]USNO, [6]Tohoku Univ. Japan

Conf. Milky Way Halo, Bonn 2007, Poster N. 39

Introduction

The outer region of the Milky Way, beyond the disk systems, has long been thought of as a single entity, comprising old stars and globular clusters that represent the earliest populations of objects to have formed in our Galaxy. Previous studies of the halo have been limited by the small numbers of stars that could be confidently identified as members, and also by the lack of available spectroscopy from which radial velocities and estimates of atmospheric parameters (such as temperature, surface gravity, and metallicity) could be obtained. Based on medium-resolution spectroscopy for 20,366 stars within a local volume of the Galaxy surrounding the Sun (obtained with the Sloan Digital Sky Survey; SDSS), we show here that the halo is clearly divisible into two broadly overlapping structural components (Carollo D. et al., 2007). These are: (1) the inner halo, which is dominated by stars on highly eccentric orbits and exhibits a peak metallicity [Fe/H] = −1.6, as well as a flattened density distribution with a zero or small net prograde rotation, and (2) the outer halo, which includes stars that have a wide range of orbital eccentricity (including many on low-eccentricity orbits), exhibits a peak metallicity [Fe/H] = −2.2, and a spherical density distribution with a highly statistically significant net retrograde rotation. Comparison with a much smaller *in-situ* sample of distant blue horizontal-branch stars (also selected from SDSS), and located between 5 and 100 kpc from the Galactic centre, provides clear supporting evidence for a change in the metallicity distribution of halo stars with distance. These results confirm expectations, based on the hierarchical galaxy assembly paradigm, that much of the outer halo of our Galaxy is likely to have been accreted from smaller sub-systems, perhaps similar to recently discovered low-luminosity dwarf spheroidal galaxies.

1.0 Calibration Stars in SDSS-I DR-5

Our sample consists of about 25,000 stars selected as calibration objects (used for providing checks on the spectrophotometric flux and telluric calibration) from SDSS-I DR-5. These stars are primarily F- (and early G-type) turnoff stars in the thick disk and halo populations of the Galaxy. Their color-based selection ensures that an adequate number (several thousand) of very low-metallicity ([Fe/H] < -2.0) stars exist. Accurate estimates of radial velocity, metallicity, temperature, surface gravity, and distance are obtained for all of these stars by application of the (still evolving) SDSS/SEGUE Spectroscopic Parameter Pipeline (SSPP)

1.1 Selection Criteria for the Kinematic Analysis

In order to obtain the best available estimates of the kinematics and orbital parameters of the stars in our sample as a function of [Fe/H] we have considered only stars satisfying the following cuts:

- **Selection** of the stars with temperature range **5000 K < Teff < 6800 K**, over which the SSPP is expected to provide the highest accuracy in both the atmospheric parameters and chemical composition → **19,687** stars

- **Local sample**: selection of stars with presents distances d < 4 kpc from the Sun and 7 < R < 10 kpc (where R is the Galactocentric distance of a star projected onto the Galactic plane). In this way we restrict the kinematical and orbital analysis to a local volume, and we limit the increase in errors in the derived transverse velocity.

After these cuts are applied, we are left with a sample of ~ **11,458 stars**, all of which have available estimates of proper motions based on the recalibrated USNO-B2 catalog. This sample is thus some **10 times** that of the formerly largest sample of non-kinematically selected thick disk and halo stars discussed in the literature (Chiba & Beers 2000 sample).

2.0 Distribution of the full sample of 20,366 unique SDSS stars in the Z-R plane

The dashed blue line represents the Galactic plane, while the filled orange dot is the position of the Sun, at Z = 0 kpc and R = 8.5 kpc. The "wedge shape" of the selection area is the result of limits of the SDSS footprint in Galactic latitude. The red points indicate the 11,458 stars that satisfy our criteria for a "local sample" of stars, having 7 kpc < R < 10 kpc, with distance estimates from the Sun d < 4 kpc, and with viable measurements of stellar parameters and proper motions.

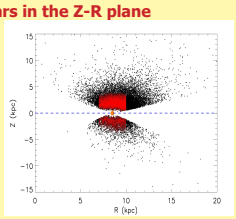

3.0 Evaluation of Kinematic Parameters

Proper motions are obtained from the re-calibrated USNOB-2 catalog, typical accuracy of ~ 3-4 mas/yr (Munn et al. 2004). These are used in combination with the measured radial velocities and estimated distances in order to obtain the full space motions (U,V,W) of the stars relative to the Local Standard of Rest (LSR). We have obtained also the rotational velocity component of the star motion around the Galactic center. The orbital parameters, such as, peri-galactic and apo-galactic distances, eccentricity and Z_{max} were derived adopting an analytic Stackel-type potential.

The U, V, and W components of the space motions of stars in our sample as a function of [Fe/H]. In all the three panels is clearly visible the thick disk and metal-weak tick-disk populations (−1.2 < [Fe/H] < −0.3), and dispersion in velocities of around 40-50 km/s. At metallicites below [Fe/H] ~ −1.2, the large velocity dispersions (on the order of 100-150 km/s) observed in each component are associated with the broadly overlapping inner- and outer-halo populations of stars.

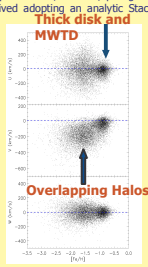

4.0 Toomre Energy Diagram

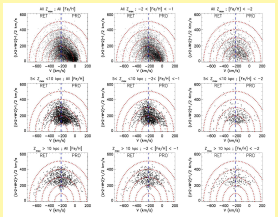

Toomre energy diagrams for various cuts of our sample on Z_{max}, and on metallicity, [Fe/H]. The blue dashed line indicates the division between retrograde (RET) and prograde (PRO) orbits with respect to the Galactic centre (assuming the LSR rotates at 220 km/s). The red dotted lines indicate total space velocities of the orbits, in the frame with respect to the Galactic centre; between 100 km/s (inner-most) and 500 km/s (outer-most). Upper row: stars exploring all ranges of Z_{max} and various cuts in [Fe/H] are shown – the left-most panel shows stars of all metallicities, the middle and right panels are for stars with intermediate (−2.0 < [Fe/H] < −1.0) metallicities, and very low metallicities, [Fe/H] < −2.0, respectively. Inspection of this row shows the decreasing importance of stars on disk-like orbits (the highly prograde stars near 0 km/s) with declining [Fe/H]. In the middle panel the majority of stars are associated with a prograde rotation inner-halo population. In the right-hand panel one can appreciate that the stars with retrograde orbits explore to much larger energies than the prograde stars. The orbits of the retrograde stars are also more uniformly distributed in energy than those of the prograde stars, which concentrate in the region of this diagram corresponding to lower orbital energies. The middle panels show the same cuts on metallicity but for intermediate cuts on Zmax, 5 < Z_{max} < 10 kpc. Still clear the contrast between high orbital energies of the stars on retrograde orbits with the lower orbital energy stars on prograde orbits. Stars in these intervals of Z_{max} are contributed from both the inner- and outer-halo populations. The lower panels show the same cuts on metallicity but for stars reaching Z_{max} > 10 kpc, which are dominated by stars from the outer-halo population. The relative contributions of stars on various energy orbits is now much more evenly distributed between retrograde and prograde orbits, independent of [Fe/H]. The V velocities of the retrograde orbits explore to much lower V than the prograde orbits explore to higher V.

5.0 Distribution of [Fe/H] for various cuts in V velocity

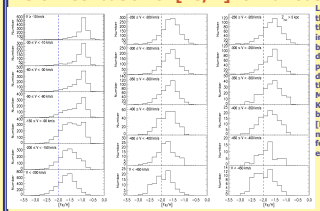

Left end column: full data set. Note that the upper three panel are dominated by thick-disk and MWTD populations (peak in [Fe/H] ~ -0.9). For V < -90 km/s becomes evident the transition to dominance by inner-halo and outer-halo populations. In the bottom panel the distribution appears similar to what in the past was considered the "Halo". Middle column: just stars with V < -200 Km/s and various cuts. Note that as V becomes increasingly retrograde, the [Fe/H] distribution shift to include larger number of stars with [Fe/H] < -2 and fewer stars with [Fe/H] ~ -1.5. Right end column: same velocity cuts as in the middle panel but for stars with Z_{max} > 5 kpc. Here the increasing dominance of stars with [Fe/H] < -2 is more apparent. In both middle and right end columns of plots, the distribution of the metallicity becomes bi-modal for V < -450 km/s.

6.0 Distribution of [Fe/H] for various cuts on the paramete $(U^2 + W^2)^{1/2}$

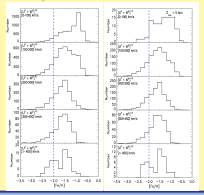

Left-hand column, the full data set is considered. Note the clear peak in the upper panel around [Fe/H] ~ −0.9 associated with the low-energy orbits for stars in the thick-disk and metal-weak thick-disk populations. The intermediate energy orbits in the middle panels of this column illustrate the increasing contribution from the inner-halo stars, with a clear peak in the metallicity around [Fe/H] ~ −1.5 emerging. There is evidence for a skewed distribution of [Fe/H] to lower values as energy increases, becoming bi-modal at the highest energies. In the right-hand column, the same cuts in energy are applied, but only for stars with Z_{max} > 5 kpc, which effectively eliminates stars with disk-like orbits, Note that for the higher energy orbits, the tail of stars with [Fe/H] < −2.0 becomes stronger, until it becomes bi-modal in the lowest panel.

7.0 Distribution of [Fe/H] for stars on highly retrograde

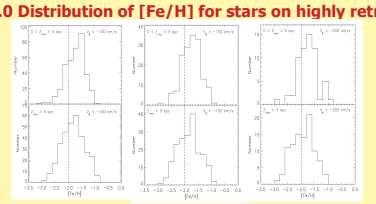

Here various cuts in V_Φ and Z_{max} are considered. Left-hand column applies for stars with V_Φ < −100 km/s; the clearly skewed distribution of [Fe/H] exhibits an increased contribution from lower metallicity stars as one progresses from the low (Z_{max} < 5 kpc) to the high (Z_{max} > 5 kpc) sub-samples. Simultaneously, the predominance of stars from the inner-halo population, with [Fe/H] ~ −1.5, decreases in relative strength, and shifts to somewhat lower [Fe/H]. Similar behaviours are seen in the middle and right-hand columns, which correspond to cuts on V_Φ < −150 km/s and −200 km/s, respectively. In the lower panels of the right-hand column, the stars with [Fe/H] < −2.0 constitute over 40% of the total samples.

8.0 [Fe/H] and orbital eccentricity

The Relationship between [Fe/H] and the orbital eccentricity for the sample of 11,458 SDSS calibration stars considered in the present analysis. Bottom left of the panel: we can clearly distinguish the presence of moderate metallicity (−1.3 < [Fe/H] < −0.3, with a mode [Fe/H] ~ −0.9), low-eccentricity (0 to 0.4) stars of the thick-disk and metal-weak thick-disk populations. Right of the panel: we can also discern the presence of low-metallicity (−2.0 < [Fe/H] < −1.0, with a mode [Fe/H] ~ −1.5), high-eccentricity (0.6 to 1.0) stars which we associate with the inner- halo population; additional members of the inner-halo population extend over all eccentricities and metallicities. The outer-halo population exhibits a relatively uniform distribution of orbital eccentricities over the full range from 0.0 to 1.0, and is dominated by lower metallicity stars (−1.5 to −3.5, with a mode [Fe/H] ~ −2.0); as a result it is not easily separated from the other populations shown in this diagram.

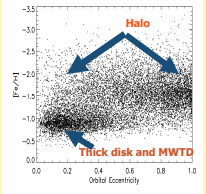

9.0 Distribution of [Fe/H] for various cuts on the orbital eccentricity

Left column: all distances from the Galactic plane are considered. At low eccentricity, it is clearly visible the thick-disk and MWTD stars. As eccentricity increases, the influence of the disk-like stars decreases, and eventually, at high eccentricity, one recovers a metallicity distribution similar to the "canonical halo"; these stars are dominated by the contribution of the inner-halo population. In the right-hand column, only those stars with Z_{max} > 5 kpc are shown, which effectively eliminates any stars from the disk-like populations. The behaviour at low eccentricity is clearly very different, as one sees a bi-modal distribution in upper panel, transitioning to a distribution with peak [Fe/H] ~ −1.5 at high eccentricity, but with long tails extending to lower metallicity. At intermediate eccentricities, the distribution of [Fe/H] exhibits characteristics of a mixture of populations with different metallicity distributions.

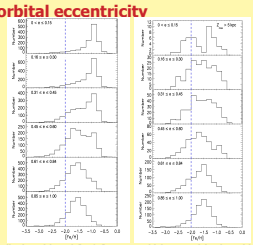

10.0 Nature of the orbits

Left column: pericentric distance vs [Fe/H] and different cuts in V_Φ. The upper panel is dominated by inner halo stars which penetrate the region near Galactic center. At more retrograde orbis the fraction of stars that penetrate the Galactic center decreases.
The most high retrograde stars which are dominated by the outer halo exhibits rperi > 6 kpc. Right column: apocentric distance. The first panel shows that the inner halo stars do not posses orbit that take them beyond ~ 15-20 kpc. This trend becomes more evident at higher retrograde orbits.

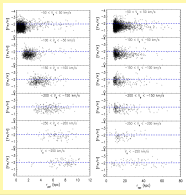

11.0 Equidensity contours

Reconstructed global density distribution in the Z-R plane for various cuts in [Fe/H].
The halo is more flattened for halo stars in the metal rich range (axis ratio ~ 0.6-0.7) whereas the most metal poor range of the halo is nearly spherical (axis ratio ~ 0.9).
The inner-halo population is characterized as a flattened density distribution that dominates for stars with [Fe/H] > -2.
The outer halo population is spherical, dominates at larger distances and for stars with [Fe/H] < -2.

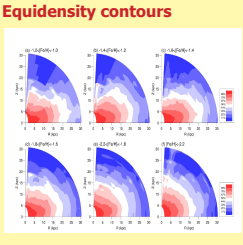

12.0 Further Confirmation of the existence of the Outer-Halo: An in-situ sample of FHB stars from SDSS

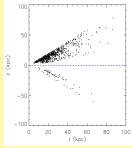

Distribution in the Z-r plane of an in-situ sample of blue horizontal-branch stars selected from SDSS DR-5

Metallicity distribution function (MDF) for different cuts in the distance from the Galactic center.
Note:
- Bi-modal distribution (upper panel) for stars within r < 10 kpc.
- Overlapping distribution of [Fe/H] at intermediate distances 10 < r < 20 kpc
- MDF almost uni-modal at 20 < r < 30 kpc
- Bi-modal again at r > 30 kpc due to the presence of inner-halo stars with highly eccentric orbit

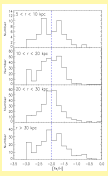

13.0 Net Rotation of the Outer-Halo

Stars at Z_{max} > 5 kpc					Stars at Z_{max} > 10 kpc			
[Fe/H] range	N_{stars}	V_{rot} (km/s)	Error		[Fe/H] range	N_{stars}	V_{rot} (km/s)	Error
-1.00 / -2.00	2041	-43.	7.		-1.00 / -2.00	554	-75.	16.
-2.00 / -5.00	549	-46.	14.		-2.00 / -5.00	231	-61.	27.

14.0 Possible scenario for the formation of Inner-Halo and Outer-Halo Populations

Inner-Halo:

- Energy dissipation of pre-Galactic gas via radiative cooling, resulting in a coherent contraction of the system as a whole, e.g., the ELS model, but *here applied exclusively to the inner-halo component.*

- *Infall of a massive satellite Galaxy into a pre-existing massive dark halo* during the process of its hierarchical clustering. Such a massive satellite would be able to reach the innermost part of a dark halo through dynamical friction, where it is finally disrupted by the tidal force of the dark halo, and leaves an inner flattened halo with stars on highly eccentric orbits.

Outer-Halo:

- The outer halo exhibits a net retrograde rotation and different distribution of orbital properties. This suggests that *the formation of the outer halo is distinct from that of both the inner-halo and disk components.*

- The outer-halo component has been formed through *dissipationless chaotic merging of smaller sub-systems with a pre-existing dark halo.*

- These sub-systems have lower mass (and low metallicity) and are subject to tidal disruption in the outer part of a dark halo.

- The surviving counterparts of such sub-systems could be similar to the *currently observed low luminosity dwarf spheroidal galaxies surrounding the Galaxy (Belokurov et al. 2006)*

What next?

- We can now target outer halo stars in order to elucidate their chemical histories ([alpha/Fe],[C/Fe]), and possibly their accretion histories.
- We can now preferentially SELECT outer-halo stars based on proper motion cuts in the local volume (SEGUE-II)
- We can take advantage of the lower [Fe/H], in general, of outer-halo stars to find the most metal-poor stars. Note that ALL the three stars with [Fe/H] < -4.5 have properties consistent with outer-halo membership.
- Constrain models for formation/evolution of the Galaxy that take all of the chemical and kinematical information into account (e.g. Tumlinson 2006).

References

Carollo D. et al, (2007), "The Dichotomy of the Galactic Halo of the Milky Way", Nature, submitted
Chiba, M. & Beers, T.C. (2000), "Kinematic of metal-poor stars in the Galaxy. III. Formation of the stellar halo and thick disk as revealed from a large sample of non kinematically selected stars", AJ, 119, 2843
Frenk, C. S., & White (1980), S.D.M. The kinematics and dynamics of the galactic globular cluster system, Mon. Not., 193, 295
Munn, J. et al. (2004), "An improved proper- motion catalog combining USNO B and the Sloan Digital Sky Survey", AJ, 127, 3034